

# Viable Gestures for Fingertip Workspace HID

Brendan P. Beauchamp

*Department of Engineering*

*Grand Valley State University*

Grand Rapids, Michigan

beauchab@mail.gvsu.edu

**Abstract**— This paper investigates seven sEMG spots and Fingertip Joint Angles recorded by Jarque Bou et al for the application of sEMG to Human Interfacing Devices (HID). Such technology is termed Gesture Computer Interfacing (GCI), and has been shown feasible through the devices such as CTRL Labs interface, and models such as those of Sartori, Merletti, and Zhao. Muscles under sEMG spots in this dataset and the actions related to them are discussed, along with what muscles and hand actions are not visible within this dataset. Viable gestures for detection algorithms are discussed based on the muscles discerned to be visible in the dataset. Detection and isolation of such viable actions is fundamental to designing an EMG driven musculoskeletal model of the hand needed to facilitate GCI.

**Keywords**— *GCI, Musculoskeletal Modeling, HID, sEMG, SHFT, CYBERGLOVE I*

## I. Introduction

Human Interface Devices (HID) refer to devices which use USB-HID protocol to allow a user to control a computer [27]. While these devices can be as simple as a mouse and keyboard, modern HID such as voice recognition apply biophysical signal modeling to increase the information bandwidth between a user and a device. Given that the hand is one of human's most evolved morphological attributes, interest was taken in Jarque Bou et al's development of a dataset recording surface electromyographic (sEMG) activity of the forearm and fingertip joint angles performing the Sollerman Hand Function Test (SHFT) [1]. This research applies modern developments in EMG Driven Musculoskeletal Modeling and simulation of the fingertip workspace to the Jarque Bou dataset in order to better understand what fingertip workspace actions may be visible from forearm sEMG [2]. Such use of sEMG for HID has been shown by companies such as CTRL Labs to be viable for Gesture Computer Interfacing (GCI) [3], the conglomerate of personal research published on this topic aims to be open source development of such a tool [4].

When a muscle contracts, signals representative of the movement known as action potentials descend from an alpha motor neuron in the ventral root of the spinal cord down to individual muscle cells known as myofibrils. The neuron, and all of the myofibrils which it innervates constitute the fundamental unit of the neuromuscular system known as Motor Units [5]. When a motor neuron transmits an action potential, contraction of all innervated myofibrils occurs at once in a phenomenon known as a Motor Unit Action Potential (MUAP) which amounts to a muscle twitch. Forearm muscles contain tens to hundreds of motor units, whose quantal and wave summation lead to graded contraction and smooth movement [9].

Action potentials descend from alpha motor neurons as intracellular action potentials (IAP) to the muscle they innervate through the release of acetylcholine (ACH) from the terminal bouton of the neuron onto the muscles' motor end plates. ACH reacts with nicotinic ACH receptors on the motor end plate, triggering sodium influx into the myofibrils. This sodium influx generates an action potential on the myofibrils, which travels to the transverse tubules of the cell and activates DHP receptors causing calcium influx from the sarcoplasmic reticulum to the sarcomere. Calcium presence induces the cross bridging cycle and causes contraction of the muscle cell [9]. sEMG is modeled linear combination of MUAP deep and proximal to the electrode, and gaussian noise representative of electromagnetic interference, motion artifacts, and other unintentionally acquired bioelectric signals. With proper electrode placement, sEMG has been shown to effectively drive physiologic models of humans through the DEMOVE grant project [5].

Using sEMG for such interfacing devices is intuitive because the technology is non invasive, and can therefore be implemented as a wearable device. Such sensors can be easily applied to measure large, superficial muscles up to approximately two centimeters below the surface of the skin. Disadvantages of the technology are its nonlinear nature, noise, and the presence of motion artifacts [5]. Furthermore, due to sEMG recording electrical activity deep to the electrodes, many muscles are superimposed upon one another in each recording within the Jarque Bou Dataset. It is therefore imperative to the development of GCI that viable muscles and their respective actuation of the fingertip workspace are outlined, and the location from which they are optimally measured is discerned.

## II. METHODS

### A. Jarque Bou Dataset

Jarque Bou investigated optimal sEMG recording of the forearm in order to calibrate seven optimal recording locations for the forearm used in the dataset [6]. Forearm regions with similar sEMG activity are shown below in figure 1.a, while the final recording spots are shown in figure 1.b. Figure 1.c shows anatomical landmarks used to locate these recording spots [2,6]. In order to record joint angles in this study, the CYBERGLOVE I was utilized to record the fingertip workspace in eighteen degrees of freedom [7]. The fingertip workspace and sEMG spots are recorded for 20 patients and 26 ADL of the SHFT. The SHFT Apparatus (a) and the CYBERGLOVE I (b) are shown below in figure 2.

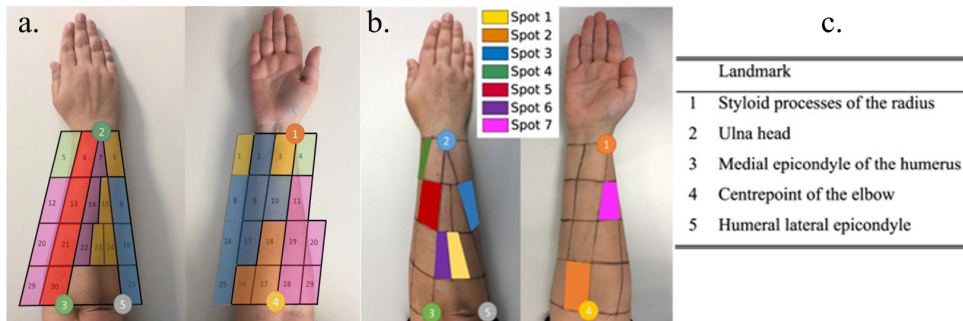


Figure 1: sEMG Recording Spots and Anatomical Landmarks



Figure 2: SHFT Apparatus and CYBERGLOVE I

### B. Actuation of the Fingertip Workspace

Joint angles between bones are controlled through bilateral pairs of muscles producing contractile forces opposing one another at the joint. Moment arms are perpendicular linearizations of rotational force which a muscle contributes to an axis of rotation. The sum of the forces opposing one another at a joint angle is known as its moment, and informs the direction of angular motion caused by muscular action [5, 8, 9]. For example, shown below in figure 3 is the wrist being actuated by flexors and extensors. Force generated by the wrist flexors is greater than extensors leading to the larger moment arm shown. Because the flexor moment arm is greater than the extensor, the moment causes the joint angle to decrease.

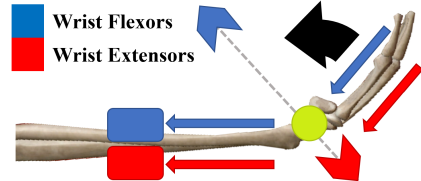


Figure 3: Moment Arms of Wrist Flexors and Extensors

Functionally, the hand actions originating from forearm muscles can be differentiated as shown in figure 4. Sartori et al designs the interaction between muscles and the conformation of the limb it acts on through principal vectors of tension from the origin of the muscle to its insertion on the distal bone [5,14-18]. Tensile forces of muscles counteract one another at joints, the derivation of this relation is known as its kinematics. A joint's axes constitute unique degrees of freedom (DOF) in the model and muscle forces change the angle at these DOF [19]. In the language of physiology, the direction of angle change constitutes which muscles are considered flexors, extensors, or opposers (Abductors and Adductors) [10].

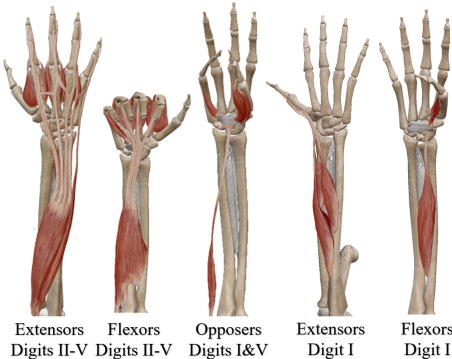


Figure 4: Hand Functional Groups in Forearm

Ensemble flexion and extension of Digits II-V is actuated largely by the digitorum muscles, and is easily measured using sEMG from the forearm [4, 6]. While opposition is actuated by the thenar and hypothenar muscles originating from the transverse carpal ligament, it is also actuated by the palmaris longus superficial to the flexor digitorum and deep to the bicipital aponeurosis and can therefore be measured from the forearm [10]. Further muscle groups observable from the forearm are Digit I flexion and extension, supination and pronation, and wrist actuation. Index finger extension may be observable with the use of HD-sEMG, but the muscle is deep to the forearm, and therefore the measurement of its actuation is impeded by the muscles superficial to it. Missing from this model are muscles of the hand, such as the lumbricals originating from the volar interosseous of the metacarpals and inserting into the sheaths of the terminal flexor digitorum and extensor expansions [10, 11]. These muscles aid in fine motor control of the hand, but their measurement would be unwieldy for a subject because sensors would have to be on their hands.

### C. Modeling of Fingertip Workspace

In order to model the Fingertip Workspace in real time, a Musculoskeletal Model is needed to drive simulation of Musculotendon Kinematics [5]. Therefore, one of the most significant developments to fingertip workspace modeling was the creation of the ARMS Lab BioSim model [11]. While the benefit of sEMG driven musculoskeletal models proposed by Merletti et al is that they can be reduced for embedded processing [5], several stages of development stand in the way of developing a model of similar caliber to their lower body model [14-18]. These stages are visualized below in figure 5. Primarily, the Cyberglove 1 used to record joint angles by Jarque Bou et al records the fingertip workspace in 18 DOF, while the ARMS Lab model describes the hand in 23 DOF. The conversion method between these two models is known as a Denavit-Hartenberg transformation, and has not been investigated in this research [19]. Furthermore, due to the proximity of muscles within the forearm, neural drives for many actions of the hand are recorded from the same SEMG spot. This summation abstracts muscular activation, and therefore must be either differentiated into muscular activation, or used in conjunction with other signal processing methods to describe activation without direct muscular activation input. It is therefore important to the development of sEMG Driven Musculoskeletal Simulation that optimal recording sites are chosen, and that the muscles within these spots are accurately mapped to the ARMS Lab model.

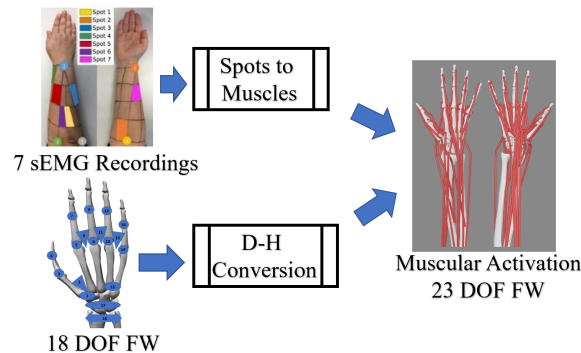


Figure 5: Jarque Bou Dataset as Input to ARMS Lab Model

Several other methods for further analysis of a single sEMG signal include Activation Enveloping, and Median Frequency Analysis. In Median Frequency Analysis power spectra are sampled from the data, and the half power point is defined as the median frequency. As muscular activation is frequency modulated by motor neurons, median frequency can provide insight into which motor units are active, the fatigue of motor units, and the intensity of a task. Thongpanja et al has shown correlation between median and mean frequency of the bicep and flexor pollicis longus with joint angle [13], while the differentiation between pinching and grasping hand conformations using the Jarque Bou dataset has been shown by Beauchamp et al through the application of activation envelopes from a single sEMG recording [4]. While these research show that more information than activation can be obtained from low dimensional sEMG recordings, further studies are required to direct activation to the ARMS lab model.

### III. RESULTS

#### *A. Neuromuscular Control - Jarque Bou Dataset*

In order to interpret sEMG recorded in the Jarque Bou Dataset for their relation to neuromuscular control of the hand, recording spots from the Jarque Bou Dataset were analyzed for likely muscles contributing to each sEMG signal. Jarque Bou et al proposed likely muscles which constitute the majority of the observed signal at each spot, these muscles are labeled with check marks in table 1 below. Furthermore, because these signals have been physically identified by forearm landmarks, muscles underneath these landmarks have been labeled with an asterisk in table 1 for further research into signal contribution. Volumetric models of the forearm were observed in the Visible Body platform for observation of muscles underneath electrode spots.

Groupings of sEMG spots are likely to record the same muscles due to the volume conductor effects of the forearm. The signal at spot 1 was stated by Jarque Bou to be largely composed of the Extensor Carpi Ulnaris [2, 6]. This makes sense because it is a superficial muscle and has a large number of motor units [4,10]. Cross talk at this source likely comes from muscles actuating digits III-V due to its location on the forearm, despite this, some muscles such as the APL and EPL which contribute to thumb actuation and radial adduction may also contribute to this signal. Furthermore, spot 6 which likely measures wrist extension and ulnar deviation is likely to contain artifacts of spot 1 due to the proximity of the sensors. Spots 5 and 6 are likely to record mutual sources originating near the interosseous of the ulna and radius and actuating near digit I.

Special care should be taken in the placement of electrodes at spots 5-7 due to their proximity to the brachioradialis. The muscle will cause significant interference with electrodes in this range due to its high number of motor units and proximity to the surface of the skin. Similarly, electrode three should be placed on the dorsal side of the interosseous crest to focus the signal on digital flexors. Digital flexors are visible from spot 3 due to the hand having few muscle bellies on the dorsal side of this region of the forearm, and most of the activation group is seen on the palmar forearm. Spot 2 observes wrist flexion at the origin of the digital flexors, the flexor carpi radialis is superficial, and it is therefore measured from this point instead.

Through experimentation with a Myoware Muscle Sensor, it was noted that spot 3 exhibits significant interference from the Extensor Digiti Minimi [4, 26]. Spot 3 was chosen to be placed on the dorsal side of the interosseous crest of the ulna to measure forearm flexion, yet in previous work it was shown to have a significant activation region on the palmar side of the forearm as well [24]. Further care should be taken in the placement of electrodes for spot 3 in order to reduce interference from extensors.

Table 1: Muscles Under sEMG Spots; Mutual (✓), This Research(\*)

Muscle	Spot 1	Spot 2	Spot 3	Spot 4	Spot 5	Spot 6	Spot 7
APL	*			✓		*	
BR				*			✓
ECRB				*	*		✓
ECRL				*			✓
ECU	*		*			✓	
EDC	*				✓	*	
EDM	*		*			*	
EI					*		
EPB				✓	*		
EPL	*		*	✓	*	*	
FCR		✓	*				*
FCU	✓		*				
FDP		*	✓				
FDS		*	✓				
FPL			✓				*
PL		✓					
PT		*					✓

Continuing from the work shown above in table 1, table 2 below shows the actions related with each EMG spot. This table is notable for future use of this dataset, as it outlines bilateral

pairs for finger flexion and extension in spots 3 and 5, thumb flexion and extension in spots 4 and 5, and wrist control abstracted through spots 1,2,6, and 7. Bilateral control of radial and ulnar deviation is observed through spot 2 (radial) and spots 1&6 (ulnar). Wrist flexion and extension is controlled bilaterally through spots 1 & 2 for flexion and spots 6 & 7 for extension.

Table 2: sEMG Spot and Associated Action

Spot	Actions of Muscles Identified by Jarque Bou
1	Wrist Flexion & Ulnar Deviation
2	Wrist Flexion & Radial Deviation
3	Flexion I-V
4	Extension I
5	Extension II-V
6	Wrist Extension and Ulnar Deviation
7	Wrist Pronation, Supination, Extension

### B. Correlating Gestures to Jarque Bou Dataset

Expanding upon the most likely muscles observed at each EMG spot, gestures easily differentiable using these spots will generate the greatest muscle activity in muscles directly below these sensors. Because the spots isolate bilateral wrist actuation, gestures using wrist motion will be easily detectable. Digits I-V flexion is measured from spot 3, therefore bilateral control of digit I (thumb) is not differentiable from digits II-V solely through measurement of activation of these seven spots. Despite this, opening and closing the hand is grossly observable through the activation of spots 3,4, and 5 as shown in conjunctive research to this paper [4]. Gestures differentiable from the Jarque Bou Dataset are shown below in figure 6.

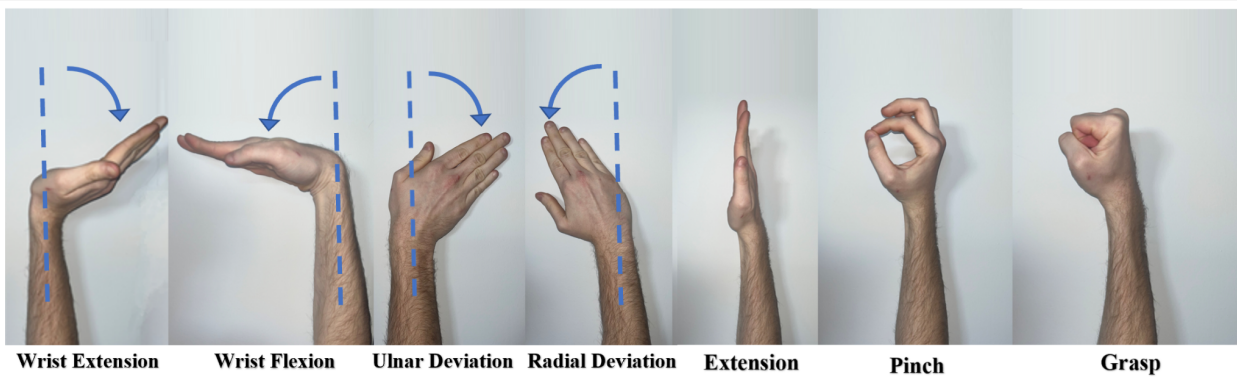


Figure 6: Differentiable Activation Jarque Bou Dataset

In Differentiation of Pinch and Grasp sEMG, the variability in the activation envelope of spot 3 has been investigated. While not directly representative of fingertip joint angles, it was shown that the intensity and frequency of activation stimulus increased with the intensity of hand

manipulation [4, 13]. Manipulating lightweight targets such as coins required significantly less muscle activation than heavy targets such as weights. Variability in activation for spot 3 as shown below in figure 7 provides opportunity to encode different intensity grasps due to the high degree of separation between task envelope distributions.

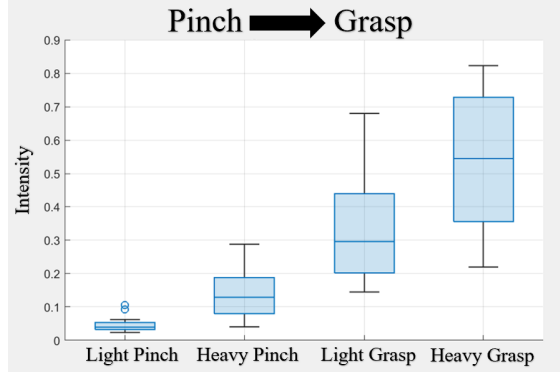


Figure 7: Activation Intensity Spot 3 (Digit Flexion) Pinch & Grasp

#### IV. DISCUSSION

This research shows that through the use of the sEMG groupings in the Jarque Bou dataset, bilateral actuation of the entire wrist, as well as digits II-V flexion and extension are visible. Due to sEMG spot 3 recording digit I-V flexion, bilateral control of digit I is not possible using activation envelopes supplied by Jarque Bou. Furthermore, ensemble study of digits II - V is required as digits cannot be differentiated from the sEMG envelopes alone. Application of this dataset to the ARMS Lab model would require similar ensemble activation of muscles as to the nature of the recordings. Further investigation to signal composition could apply coherence and entropy methods to the power spectra of the EMG to observe signal crosstalk [21]. Furthermore muscle inferences could be contributed by joint angle change and observing activation change with the model based on weights of depth and motor unit pool size.

Gestures not differentiable within this dataset are any whose bilateral control is not observed from separate EMG spots. An example of such a gesture is a peace sign, which uses the dorsal interossei between digits 1 and II to abduct digit II, and the palmar interossei to adduct digit III. These muscles originate from the proximal side of the metacarpals and insert on the extensor expansions and phalanges, therefore not observable from any of the seven sEMG spots. It is a good rule of thumb that abduction and adduction of digits will not be visible bilaterally due to their reliance on hand muscles. Pronation and Supination are not differentiable in this dataset using activation because both actions are controlled by muscles observable only from spot 7. While these actions would not be visible using muscle force, application of an accelerometer to an sEMG wristband would not only allow actuation of supination and pronation, but also create insight on limb conformation and three dimensional position.

While these gestures are not part of the SHFT, actions such as pointing with digit II or digit V may be visible from sEMG data. Extensors for these digits were observed at spots 5 and 3 using

the visible body software, and through observation on volunteers. Finger II extension is actuated from the extensor indicis likely observable from spot 5, while finger V extension is actuated by the extensor digiti minimi visible from spot 3. The lack of fingertip workspace data and SHFT tasks to observe these actions limit the development of this investigation. Future work could involve directly observing these two actions to differentiate more fingertip workspace control from forearm musculature.

The provided GitHub link is an open source repository to aid in physiologic study of the forearm through the Jarque Bou dataset [2]. Code was designed in conjunctive research to aid in the differentiation of pinch and grasp tasks using forearm sEMG. The Fingertip Workspace Atlas is a spreadsheet containing the muscles of the forearm and hand as well as their physiologic properties within multiple models of the fingertip workspace. The purpose of this research is integration of the ARMS Lab model, Hill Type Musculoskeletal Modeling, Jarque Bou Dataset, and Lower Limb EMG Driven Musculoskeletal Models by Sartori et al to generate an open source sEMG Driven Musculoskeletal Model of the forearm. This technology would aid in the development of Gesture Computer Interfacing.

Using sEMG Driven Musculoskeletal models for human interfacing devices (GCI) implies the transduction of a computational model of the hand using information derived solely from sEMG. The analysis of the Jarque Bou Dataset in this research implies a significantly lower dimensional model than that designed by the ARMS Lab. This can be circumnavigated through conversion between models, further investigation into signal extraction from the Jarque Bou Dataset, or an HD-sEMG sleeve could be designed to spatially sample the forearm using a smaller interelectrode distance in order to isolate more signals [20]. Through development of such a model, insight into hand conformation could aid in assistive technologies, protecting humans from hazardous materials testing, or improve human interfacing to complex technologies.

## V. CONCLUSION

This research observes the Jarque Bou Dataset for implementation into sEMG Musculoskeletal Modeling. The Jarque Bou Dataset is found to measure full bilateral control of the forearm, and ensemble bilateral control of digits II-V. SEMG groups were analyzed for muscles underneath them and correlated to the actions of the muscles which were most likely to contribute to measured signals. Development of this technology is not only useful for the development of assistive technologies, but imperative to streamline the control of devices which require three dimensional control. Limitations in this technology are discussed as they relate to the Jarque Bou dataset, and methods for further investigation of the fingertip workspace are introduced. sEMG Driven Musculoskeletal Modeling proposes that musculoskeletal actuation can be transduced as a vector of sEMG signals which can be used to biometrically encode motor control.

## VI. REFERENCES

- [1] Sollerman, C., & Ejeskär, A. (1995). Sollerman hand function test: A standardized method and its use in tetraplegic patients. *Scandinavian Journal of Plastic and Reconstructive Surgery and Hand Surgery*, 29(2), 167–176. <https://doi.org/10.3109/02844319509034334>
- [2] Jarque-Bou, N. J., Vergara, M., Sancho-Bru, J. L., Gracia-Ibáñez, V., & Roda-Sales, A. (2019). A calibrated database of kinematics and EMG of the forearm and hand during activities of daily living. *Scientific Data*, 6(1). <https://doi.org/10.1038/s41597-019-0285-1>
- [3] “CTRL-Labs Neural Interface Technology,” *CTRL*. [Online]. Available: <https://www.luxcapital.com/companies/ctrl-labs#:~:text=CTRL%2Dlabs%20has%20created%20a,the%20brain%20%2D%20no%20gestures%20required./>. [Accessed: 08-Feb-2021].
- [4] B. Beauchamp, “Gesture Computer Interfacing: Open Source Repository,” *GitHub*. [Online]. Available: <https://github.com/beauchab/GestureComputerInterfacing>. [Accessed: 11-Dec-2022].
- [5] R. Merletti and D. Farina, *Surface Electromyography: Physiology, Engineering, and Applications*. John Wiley & Sons, 2016.
- [6] Jarque-Bou, N., Vergara, M., Sancho-Bru, J., Roda-Sales, A., & Garcia-Ibanez, V. (2018, October 29). *Identification of forearm skin zones with similar muscle activation patterns during activities of daily living - journal of Neuroengineering and Rehabilitation*. BioMed Central. Retrieved December 6, 2022, from <https://jneuroengrehab.biomedcentral.com/articles/10.1186/s12984-018-0437-0>
- [7] “Cyberglove ii,” *CyberGlove Systems LLC*. [Online]. Available: <http://www.cyberglovesystems.com/cyberglove-ii/>. [Accessed: 11-Dec-2022].
- [8] Heine, R., Manal, K., & Buchanan, T. S. (2003). Using hill-type muscle models and EMG data in a forward dynamic analysis of joint moment. *Journal of Mechanics in Medicine and Biology*, 03(02), 169–186. <https://doi.org/10.1142/s0219519403000727>
- [9] S. I. Fox, *Human physiology*. New York, NY: McGraw Hill Education Create, 2022.
- [10] “Visible Body - Virtual Anatomy to See Inside the Human Body,” Visible Body. <http://www.visiblebody.com> (accessed Oct. 25, 2020).

- [10] R. Sica, A. McComas, A. Upton, and D. Longmire, "Motor Unit Estimations of Small Muscles in the Hand," *Journal of Neurology, Neurosurgery and Psychiatry (JNNP)*. [Online]. Available: <https://jnnp.bmjjournals.org/content/jnnp/37/1/55.full.pdf>. [Accessed: 10-Dec-2022].
- [11] D. C. McFarland, B. I. Binder-Markey, J. A. Nichols, S. J. Wohlman, M. de Bruin, and W. M. Murray, "A Musculoskeletal Model of the Hand and Wrist Capable of Simulating Functional Tasks," *bioRxiv*, p. 2021.12.28.474357, 2021, doi: 10.1101/2021.12.28.474357.
- [12] M. D. F. Ma'as, Masitoh, A. Z. U. Azmi and Suprijanto, "Real-time muscle fatigue monitoring based on median frequency of electromyography signal," 2017 5th International Conference on Instrumentation, Control, and Automation (ICA), 2017, pp. 135-139, doi: 10.1109/ICA.2017.8068428.
- [13] S. Thongpanja, A. Phinyomark, C. Limsakul, and P. Phukpattaranont, "Application of mean and median frequency methods for identification of human joint angles using EMG Signal," *Lecture Notes in Electrical Engineering*, pp. 689–696, 2015.
- [14] T.S. Buchanan, D. G. Lloyd, K. Manal, and T.F. Besier, "Neuromusculoskeletal modeling: estimation of muscle forces and joint moments and movements from measurements of neural command." *J. Appl. Biomech.* (2004).
- [15] P. Gerus, M. Sartori, T.F. Besier, B.J. Fregly, S.L. Delp, S. A. Banks, M. G. Pandy, D. D. D'Lima, D. G. Lloyd, "Subject - specific knee joint geometry improves predictions of medial tibiofemoral contact forces," *J. Biomech.* (2013).
- [16] D. G. Lloyd, T. F. Besier, "An EMG-driven musculoskeletal model to estimate muscle forces and knee joint moments in vivo," *J. Biomech.* (2003).
- [17] F. Sartori, D. Farnia, D. G. Lloyd, "EMG-driven forward-dynamic estimation of muscle force and joint moment about multiple degrees of freedom in the human lower extremity," *PLoS One.* (2012).
- [18] C. R. Winby, D. G. Lloyd, T. F. Besier, T. B. Kirk, "Muscle and external load contribution to knee joint contact loads during normal gait," *J. Biomech.* (2009).
- [19] J. Denavit and R. S. Hartenberg, "A Kinematic Notation for Lower-Pair Mechanisms Based on Matrices," *DH Paper*. [Online]. Available: <https://home.konkuk.ac.kr/~cgkang/courses/robotics/courseMaterials/DHpaper.pdf>.
- [20] Brendan. P. Beauchamp et. al, "MicroElectrodes for High Density Surface Electromyography" *Unpublished*, Oct. 2022
- [21] E. G. Lovett and K. M. Ropella, "Time-frequency coherence analysis of atrial fibrillation termination during Procainamide administration," *Annals of Biomedical Engineering*, vol. 25, no. 6, pp. 975–984, 1997.

- [22] “Biering-Sørensen Test,” Shirley Ryan AbilityLab. [Online]. Available: <https://www.sralab.org/rehabilitation-measures/beiring-sorensen-test>. [Accessed: 15-Nov-2021].
- [23] P. A. Ortega-Auriol, T. F. Besier, W. D. Byblow, and A. J. McMorland, “Fatigue influences the recruitment, but not structure, of muscle synergies,” *Frontiers in Human Neuroscience*, vol. 12, 2018.
- [24] “Ulna,” Ulna - an overview | ScienceDirect Topics. [Online]. Available: <https://www.sciencedirect.com/topics/agricultural-and-biological-sciences/ulna>. [Accessed: 10-Dec-2022].
- [25] A. T. Nguyen, J. Xu, M. Jiang, D. K. Luu, T. Wu, W.-kin Tam, W. Zhao, M. W. Drealan, C. K. Overstreet, Q. Zhao, J. Cheng, E. W. Keefer, and Z. Yang, “A bioelectric neural interface towards intuitive prosthetic control for amputees,” *bioRxiv*, 01-Jan-2020. [Online]. Available: <https://www.biorxiv.org/content/10.1101/2020.09.17.301663v1.full?ref=.> [Accessed: 10-Dec-2022].
- [26] “MYOWARE 2.0 Muscle Sensor,” *MYOWARE by Advancer Technologies*, 01-Apr-2022. [Online]. Available: <https://myoware.com/products/muscle-sensor/>. [Accessed: 10-Dec-2022].
- [27] Mhopkins-Msft, “Introduction to human interface devices (HID) - windows drivers,” Windows drivers | Microsoft Learn. [Online]. Available: <https://learn.microsoft.com/en-us/windows-hardware/drivers/hid/>. [Accessed: 10-Dec-2022].
- [28] E. Peña-Pitarch, N. T. Falguera, and J. (James) Yang, “Virtual human hand: model and kinematics,” *Computer Methods in Biomechanics and Biomedical Engineering*, vol. 17, no. 5, pp. 568–579, Apr. 2014, doi: 10.1080/10255842.2012.702864.
- [29] Brendan. P. Beauchamp et. al, “A Low Cost sEMG Development Platform for Hand Joint Angle Acquisition” in 2020 IEEE 11th Annual Information Technology, Electronics and Mobile Communication Conference (IEMCON), Oct. 2020, doi: 10.1109/IEMCON51383.2020.9284889.